Available online at www.sciencedirect.com
ScienceDirect
Trans. Nonferrous Met. Soc. China 23(2013) 148−155
Transactions of Nonferrous Metals Society of China
www.tnmsc.cn

Thermal stability, crystallization behavior, Vickers hardness and magnetic properties of Fe−Co−Ni−Cr−Mo−C−B−Y bulk metallic glasses

Jia-jia HAN[1], Cui-ping WANG[1], Sheng-zhong KOU[2], Xing-jun LIU[1]

1. Department of Materials Science and Engineering, College of Materials, Xiamen University, Xiamen 361005, China;
2. State Key Laboratory of Gansu Advanced Nonferrous Metal Materials, Lanzhou University of Technology, Lanzhou 730050, China

Received 28 November 2011; accepted 8 May 2012

Abstract: Thermal stability, crystallization behavior, Vickers hardness and magnetic properties of the $Fe_{41}Co_{7-x}Ni_xCr_{15}Mo_{14}C_{15}B_6Y_2$ (x=0, 1, 3, 5) bulk metallic glasses were investigated. The $Fe_{41}Co_{7-x}Ni_xCr_{15}Mo_{14}C_{15}B_6Y_2$ (x=0, 1, 3, 5) metallic glasses were fabricated by copper mold casting method. The thermal stability and crystallization behavior of the metallic glass rods were investigated by differential scanning calorimetry and isothermal experiments. Hardness measurements for samples annealed at different temperatures for different time were carried out at room temperature by the Vickers hardness tester, and magnetic measurements were performed at different temperatures by the vibrating sample magnetometer. It is shown that the addition of Ni does not play a positive role for enlarging ΔT_x and GFA from parameter γ ($=T_x/(T_g+T_l)$), and it can, however, increase the activation energy in the initial stage of crystallization by changing the initial crystallization behavior. The minor addition of Ni can refine the crystal grain obtained from the full crystallization experiment. The primary crystallization causes the decrease of hardness in these alloys, and as the crystallization continues, the hardness in all samples increases instead due to the precipitation of carbide and boride. The annealing temperature has an obvious effect on magnetic properties of these alloys, and the minor addition of Ni can effectively prevent the alloy annealed at high temperature to transform from paramagnetic to ferromagnetic state.
Key words: Fe−Co−Ni−Cr−C−B−Y; metallic glass; thermal stability; annealing; magnetic properties

1 Introduction

Great attention has been focused on the Fe-based bulk metallic glasses (BMGs) because they exhibit good soft magnetic properties, high glass forming ability (GFA), and a wide supercooled liquid region before crystallization [1−11]. Since the first Fe-based BMG was reported in 1995 [12], the development of Fe-based BMG with large GFA has become an important research topic in recent years. LU et al [6] reported that the Fe-based BMG with the critical size of centimeter level for the first time can be obtained in the Fe−Cr−Mo−Mn−C−B system [6]. Later, PONNAMBALAM and POON [13] developed the $Fe_{48}Cr_{15}Mo_{14}C_{15}B_6Y_2$ BMG with the critical thickness of 9 mm, and SHEN et al [7] successfully improved the $Fe_{41}Co_7Cr_{15}Mo_{14}C_{15}B_6Y_2$ BMG with a critical thickness as large as 16 mm by the addition of 7% (mole fraction) Co. The current work found that the addition of element Ni has significant effect on the mechanism (plasticity) and soft magnetic properties in Fe-based BMG [10,11]. Many efforts have been made to enhance GFA [5−7], however, the detailed work about the other important properties such as thermal stability, crystallization behavior and magnetic properties for Fe−Co−(Ni)−Cr−Mo−C−B−Y BMG has not been reported yet.

The aim of this work is to study the properties of Fe−Co−Ni−Cr−Mo−C−B−Y BMG by the substitution of Ni for part of Co in the original Fe−Co−Cr−Mo−C−B−Y BMG system. The element Ni is chosen due to the following considerations. 1) The properties of element Ni are similar to those of Fe and Co, and there is a large negative enthalpy of mixing between Ni and other elements such as Fe, Cr, Mo, C, B and Y [14]. The strong combination between different types of atoms would lead to forming a number of types of compounds especially boride, which is favorable to forming amorphous phase

Foundation item: Project (2012CB825700) supported by the National Basic Research Program of China
Corresponding author: Xing-jun LIU; E-mail: lxj@xmu.edu.cn
DOI: 10.1016/S1003-6326(13)62441-3

during solidification [15]; 2) Ni is a ferromagnetic element like Co and Fe, and its addition could dramatically affect apparent magnetic state of the alloy. Therefore, it is attractive to study the ratios of Ni and Co on the properties of Fe−Co−Ni−Cr−Mo−C−B−Y system. Consequently, a series of Fe−Co−Ni−Cr−Mo−C−B−Y BMGs are produced to perform the study on their properties of thermal stability, crystallization behavior, Vickers hardness and magnetic properties.

2 Experimental

The $Fe_{41}Co_{7-x}Ni_xCr_{15}Mo_{14}C_{15}B_6Y_2$ (x=0, 1, 3, 5) alloys were prepared by arc melting method from the mixture of pure Fe−B (purity 99.9%), Fe (99.9%), Co (99.87%), Cr (99.98%), Ni (99.9%), Mo (99.9%), C (99.9%), Y (99.9%) under a high purity argon atmosphere. The BMG rods with the diameters of 3 mm and 6 mm were prepared from the ingots by the copper mold casting method under argon atmosphere.

The structures in the solid state were identified by analytical X-ray diffraction (XRD) experiments (Panalytical X'pert PRO) with Cu K_α radiation. The crystallization kinetics of the amorphous alloy was characterized by continuous heating differential scanning calorimeter (DSC) (Netzsch STA 404) at the heating/cooling rates of 10−40 K/min. Thermal stability and crystallization behavior were further investigated by isothermal experiments. The morphology was determined by electron probe microanalysis (EPMA) (JXA−8100). Hardness measurements for the samples annealed at different temperatures were carried out at room temperature by the Vickers hardness tester (HMV−2T) under a load of 19.614 N. Magnetic measurements were performed at different temperatures by the vibrating sample magnetometer (VSM) (VSM−5−15).

3 Results and discussion

3.1 Preparation and identification of bulk metallic glass

The typical XRD patterns obtained from the cross section of $Fe_{41}Co_{7-x}Ni_xCr_{15}Mo_{14}C_{15}B_6Y_2$ (x=0, 1, 3, 5) alloys with the diameters of 3 mm and 6 mm prepared by the copper mold casting method show the homogenous amorphous structures for the as-cast rods (Figs.1(a) and (b)), and only a broad diffraction peak centered at 2θ=38°−48° was detected. In order to further confirm the amorphous structure, the $Fe_{41}Co_{7-x}Ni_xCr_{15}Mo_{14}C_{15}B_6Y_2$ (x=0, 1, 3, 5) as-cast alloys were etched for 6 h using etching solution (V(HF):V(HNO_3)=3:1), and they all finally exhibited the homogeneous characteristic of glassy phase with no evidence of crystallization.

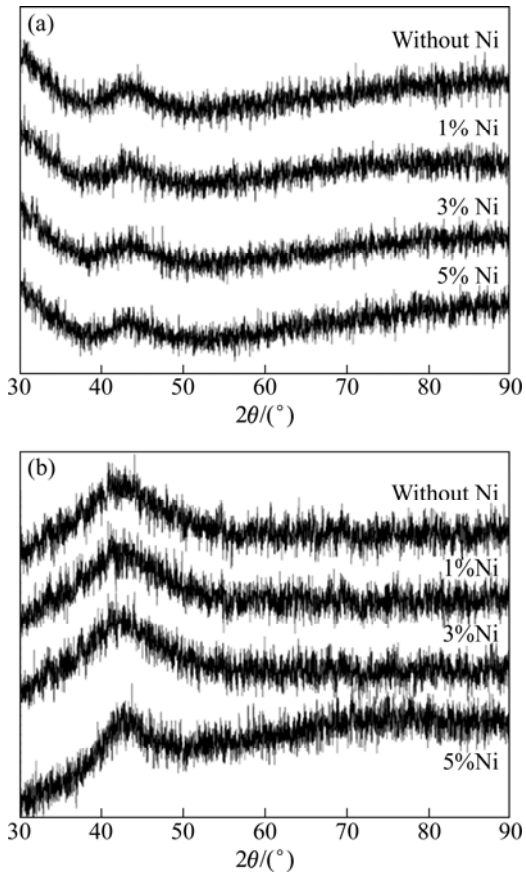

Fig. 1 XRD patterns of $Fe_{41}Co_{7-x}Ni_xCr_{15}Mo_{14}C_{15}B_6Y_2$ (x=0, 1, 3, 5) as-cast alloys with diameters of 3 mm (a) and 6 mm (b)

3.2 Crystallization kinetics and thermal stability

Figure 2 shows the continuous heating DSC curves of $Fe_{41}Co_{7-x}Ni_xCr_{15}Mo_{14}C_{15}B_6Y_2$ (x=0, 1, 3, 5) amorphous alloys at the heating rate of 10 K/min. From these curves, the glass transition temperature (T_g), onset crystallization temperatures (T_x), onset melting temperature (T_m) and liquidus temperature (T_l) can be distinctly determined. The DSC curves exhibit significant endothermic peaks related to glass transition and at least four exothermic events related to crystallization. These exothermic peaks at each heating rate present an asymmetrical profile, which indicates the occurrence of two overlapping reactions, especially for the first step of crystallization. Besides, all samples show the similar crystallization behavior at this stage. However, the temperature of the last step of crystallization obviously decreases with the increasing addition of Ni. The thermal parameters of the samples obtained at different heating/cooling rates are listed in Table 1. It can be seen that the value of T_x firstly decreases by adding 1% Ni and then increases to nearly original value by the further addition of Ni. The value of T_g monotonously decreases by the addition of Ni. The liquidus temperature, however, remains constant for all samples.

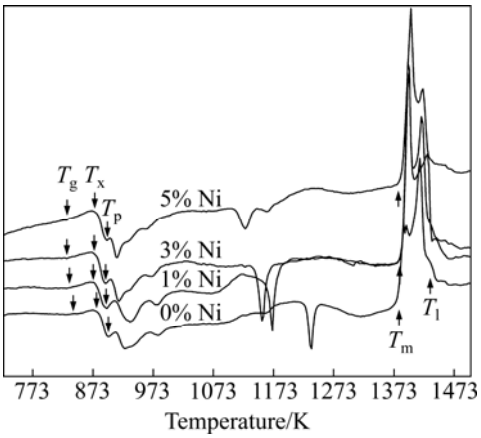

Fig. 2 DSC curves of $Fe_{41}Co_{7-x}Ni_xCr_{15}Mo_{14}C_{15}B_6Y_2$ (x=0, 1, 3, 5) BMGs with diameter of 3 mm (heating rate of 10 K/min)

In general, the GFA of metallic glass is simultaneously influenced by thermal stability and kinetic factors [16]. Some investigators have proposed many criteria to predict the GFA from various aspects [17−23]. For example, INOUE et al [20,21] suggested ΔT_x ($=T_x-T_g$), the width of the supercooled liquid region, to describe the stability of the supercooled liquid phase; LU and LIU [23] proposed a parameter γ ($=T_x/(T_g+T_l)$) as the criteria of GFA.

From Table 1, the value of ΔT_x firstly decreases by adding 1% Ni and then increases to nearly original value by the further addition of Ni. It can be concluded that the addition of Ni does not play a positive role for enlarging ΔT_x. In other words, the stability of supercooled liquid phase is not enhanced by the addition of Ni.

The parameter γ was also listed in Table 1, from which it can be seen that the variation of γ has a similar trend as ΔT_x. The variation tendency of γ indicated that the GFA is almost not affected with more than 1% addition of Ni for this system. It can be found from the value of ΔT_x that there are some corresponding relations between the width of ΔT_x and the GFA for these alloys.

The thermal stability for BMGs can be evaluated by the activation energy of crystallization. According to the peak shifts of the linear heating DSC patterns at different heating rates, the effective activation energy for the first step of crystallization can be evaluated by the Kissinger method [24] as follows:

$$\ln(\frac{T_p^2}{\varphi}) = \frac{E}{RT_p} + A \quad (1)$$

where T_p is the first peak temperature at which the primary crystallization attains its maximum value, φ is the heating rate obtained from DSC, A is temperature-independent constant, E is the apparent activation energy, and R is the gas constant.

Figure 3 shows the Kissinger plots of $Fe_{41}Co_{7-x}Ni_xCr_{15}Mo_{14}C_{15}B_6Y_2$ (x=0, 1, 3, 5) BMGs, from which the activation energy E can be obtained by plotting $\ln(T_p^2/\varphi)$ versus $1/(RT_p)$. For the first step of crystallization, the values of E were determined to be

Table 1 Thermal properties of $Fe_{41}Co_{7-x}Ni_xCr_{15}Mo_{14}C_{15}B_6Y_2$ (x=0, 1, 3, 5) alloys with diameter of 3 mm deduced from DSC measurements at different heating/cooling rates of 10−40 K/min

x	Heating rate/(K·min^{-1})	T_g/K	T_x/K	ΔT_x/K	T_m/K	T_{xc}/K	T_l/K	T_p/K	γ
0	10	838	883	45	1381	1383	1446	900	
0	20	846	898	52	1381	1377	1447	916	0.391
0	30	846	904	58	1381	1372	1447	922	
0	40	847	909	62	1381	1368	1448	929	
1	10	838	877	39	1388	1389	1447	895	
1	20	846	889	43	1388	1383	1448	906	0.387
1	30	845	895	50	1388	1377	1448	912	
1	40	846	899	53	1388	1372	1448	918	
3	10	833	878	45	1388	1387	1446	895	
3	20	841	893	52	1388	1381	1446	907	0.39
3	30	843	899	56	1388	1377	1447	914	
3	40	845	905	60	1388	1374	1448	920	
5	10	834	878	44	1388	1407	1444	896	
5	20	841	892	51	1388	1402	1444	908	0.39
5	30	843	898	55	1388	1399	1445	914	
5	40	845	905	60	1388	1395	1445	921	

415.6, 508.0, 463.8 and 470.4 kJ/mol, respectively. The maximum and minimum values (508.0 and 415.6 kJ/mol) were obtained from the $Fe_{41}Co_6Ni_1Cr_{15}$- $Mo_{14}C_{15}B_6Y_2$ and $Fe_{41}Co_7Cr_{15}Mo_{14}C_{15}B_6Y_2$ BMGs, respectively. The same results can also be obtained from the curve by plotting $\ln(T_g^2/\varphi)$ versus $1/(RT_g)$. Generally, the large GFA corresponds to the high crystallization activation energy. Nevertheless, from Table 1, the $Fe_{41}Co_6Ni_1Cr_{15}Mo_{14}C_{15}B_6Y_2$ BMG has the minimum γ (0.387) and the narrowest ΔT_x (43 K). The opposite trend of E represented here is due to the reason that the crystallization activation energy is actually determined by the stability of amorphous phase and the type of crystalline phase. The crystallization activation energy of amorphous alloy only reflects the structure difference between the primary phase and amorphous phase. The more the structure difference is, the more the value of crystallization activation energy is. Only when the primary phase is comparative on heating and quenching, the crystallization activation energy E can actually reflect the GFA of the alloy [25]. In this case, the initial phase in $Fe_{41}Co_6Ni_1Cr_{15}Mo_{14}C_{15}B_6Y_2$ BMG on heating has the most different structure from amorphous.

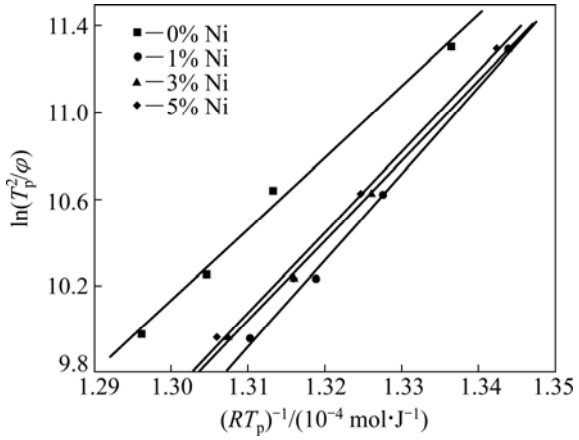

Fig. 3 Kissinger plots of T_p for all samples

3.3 Isothermal crystallization

The isothermal crystallization experiments of $Fe_{41}Co_{7-x}Ni_xCr_{15}Mo_{14}C_{15}B_6Y_2$ (x=0, 1, 3, 5) BMGs were performed at 823, 848, 873, 893, and 1273 K for 10, 30 and 60 min, respectively. The experimental results indicated that there is no obvious crystallization observed at the temperature around T_g. In order to observe the initial transformation of structure, the annealing temperature was chosen at 823 K for different times. Figure 4 shows the four XRD patterns obtained from the specimens annealed at 823 K for 10, 30 and 60 min, respectively. For the patterns for 10 min, many sharp peaks can be observed clearly. The peaks before 30° were identified as Y-compound-like phase. However, with the increase of annealing time, these sharp peaks disappear, whereas the others remain, which can be detected especially from the specimens with 1% and 5% Ni. Figure 5 shows the XRD patterns obtained from the specimens annealed at 848 K for 2 h. The specimen with 1% Ni has more smooth peaks than those with 3% and 5% Ni, which is in agreement with the conclusion from crystallization activation energy mentioned above. With the increase of annealing temperature up to 893 K, some stable phases gradually precipitate as shown in Fig. 6. It is seen that the precipitates are α-Fe and $(Fe, Cr)_{23}(B, C)_6$

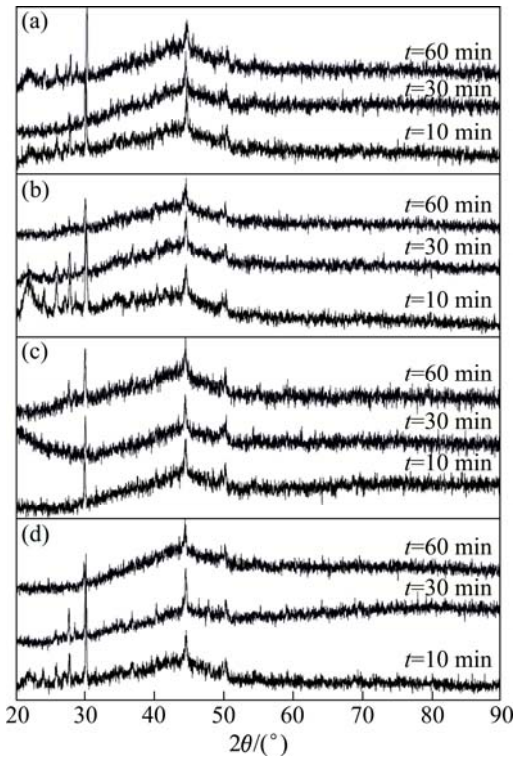

Fig. 4 XRD patterns obtained from specimens annealed at 823 K for 10, 30 and 60 min: (a) Without Ni; (b) 1% Ni; (c) 3% Ni; (d) 5% Ni

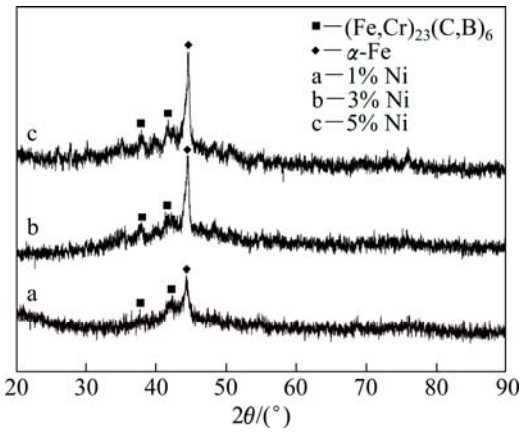

Fig. 5 XRD patterns obtained from specimens annealed at 848 K for 2 h

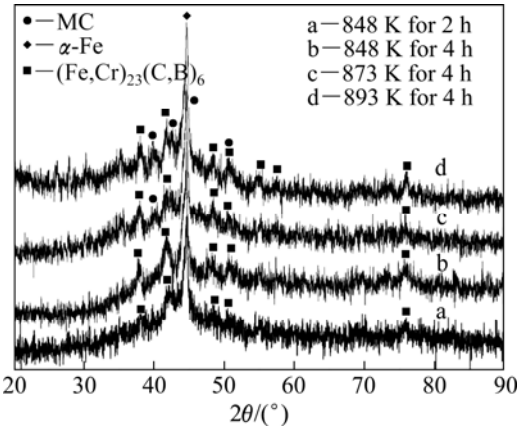

Fig. 6 XRD patterns of $Fe_{41}Co_6Ni_1Cr_{15}Mo_{14}C_{15}B_6Y_2$ alloy annealed at 848−893 K

phases at 848 K from the curves a and b in Fig. 6. Some new peaks (the curves c and d in Fig. 6) were clarified to be MC (M=Mo) phase when the sample was heated up to 873 K. The sequence of structure development could be described as follows: amorphous structure → Y-compound-like phase + α-Fe → α-Fe + $(Fe,Cr)_{23}(B,C)_6$ + MC.

Further study on the isothermal experiments was carried out at 1273 K after full crystallization. Figure 7 shows the typical microstructures which are composed of fine and uniform main phase grains of the samples annealed at 1273 K for 1 h. It can be noticed that the crystal grain of Ni-added alloy is smaller than that of Ni-free one. More evidently, the peak height reduces and the half width at half maximum becomes broad with the increase of Ni addition from the XRD patterns as shown in Fig. 8, which implies that the addition of Ni causes the further refinement of crystal grain. The consequence of grain refinement could be manifested in other properties such as magnetism that would be discussed later. The unidentified peaks at about 28° are probably generated by some other unknown phases (see Fig. 8).

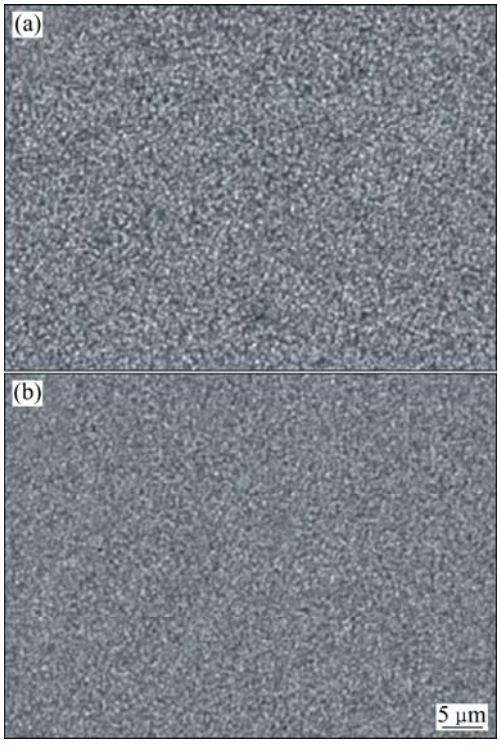

Fig. 7 Microstructures of alloys annealed at 1273 K for 1 h: (a) Without Ni; (b) 5% Ni

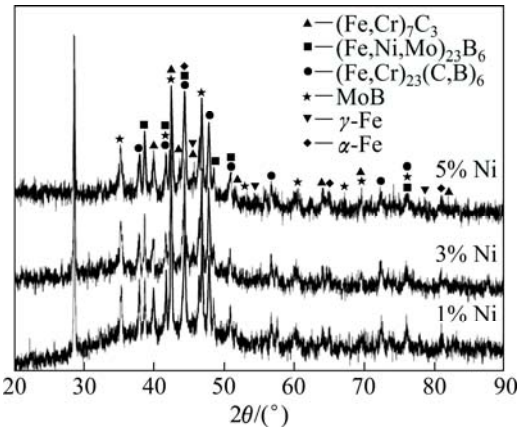

Fig. 8 XRD patterns of alloys annealed at 1273 K

In order to get an intuitive grasp of precipitation behavior, the vertical section diagram in the Fe−Cr−Mo−B−C−Y system was calculated using the Calculation of Phase Diagram (CALPHAD) method. Since the contents of Co and Ni are small, the XRD patterns are similar in all samples (Fig. 8), and the elements Co and Ni do not form individual phases but just dissolve into other phases in this system. Thus, neglecting Co and Ni in this calculation is acceptable. The calculated vertical section diagram and phase fraction diagram are shown in Fig. 9. It is found that the solidus temperature is around 1550 K, which significantly increases by about 100 K without the additions of Co and Ni elements according to the DSC results. It is thus clear that Co and/or Ni play an important role in lowering solidus temperature. From the calculated phase diagram, the α-Fe, MC (M = Mo) and $(Fe,Cr)_{23}(C,B)_6$ phases precipitate at 873 K. The MoB phase is absent in the experiment due to the kinetic factor at such low temperature. The M_7C_3, $M_{23}C_6$, M_3C, (M = Cr, Fe, Mo), BCC (α-Fe), and MoB phases precipitate at 1173−1273 K, which is in good agreement with the annealing experiment in this work. The phase fraction diagram shown in Fig. 9 denotes that the $M_{23}C_6$ and BCC (α-Fe) are the main precipitated phases within a large temperature range.

3.4 Vickers hardness test

The Vickers hardness (HV) is one of the indicators

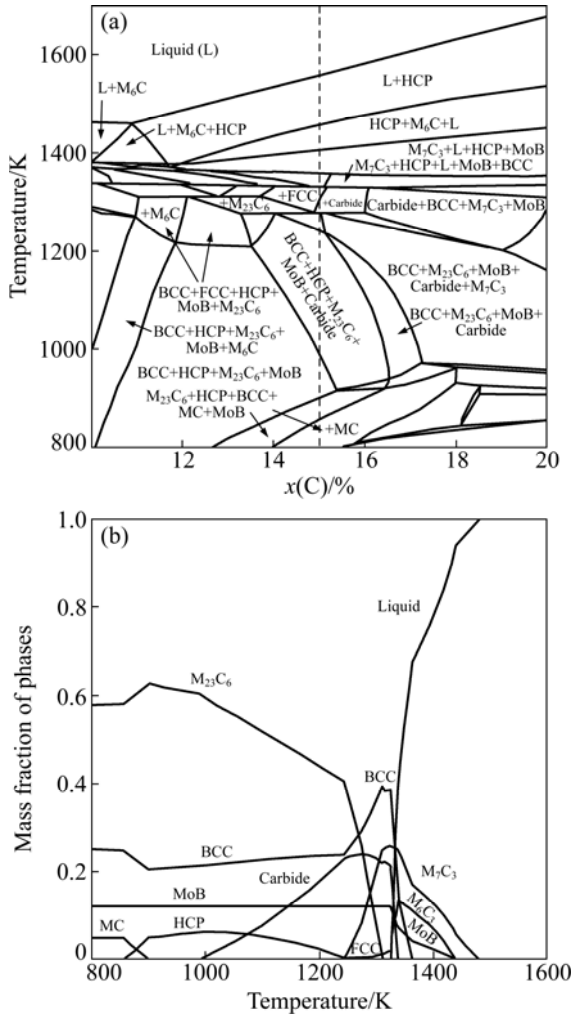

Fig. 9 Calculated vertical section diagram of $FeCr_{15}Mo_{14}B_6Y_2C$ system (a) and phase fraction diagram of $Fe_{48}Cr_{15}Mo_{14}B_6Y_2C_{15}$ (b)

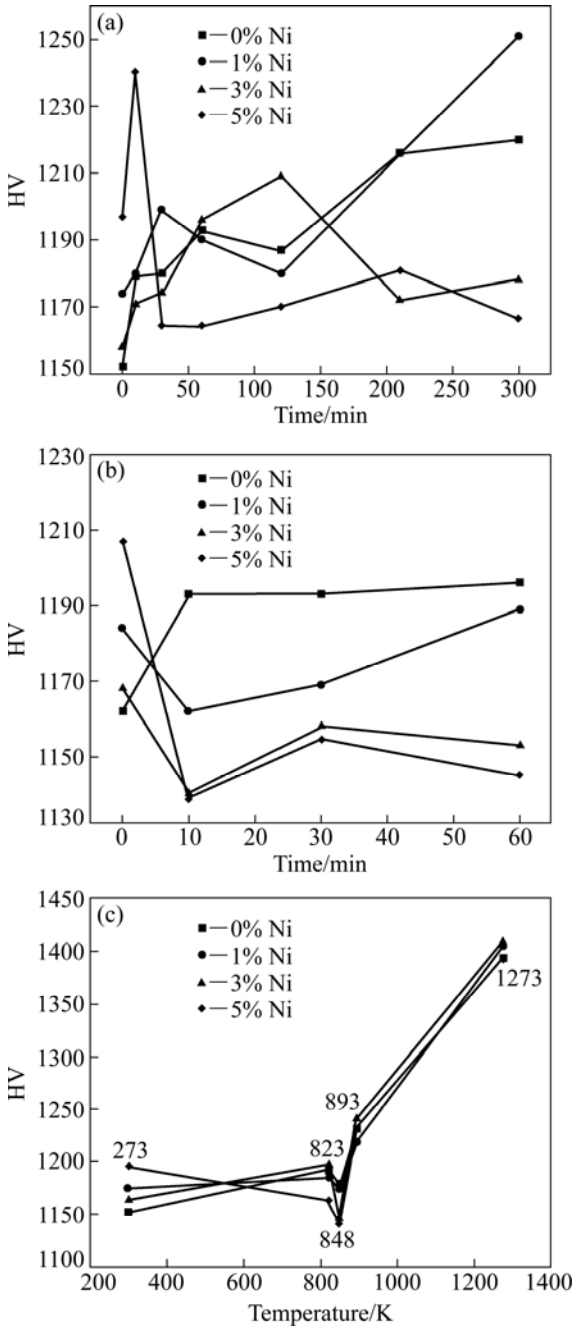

Fig. 10 Hardness of alloys annealed at 823 K (a) and 848 K (b) for different times, and annealed at different temperatures (c)

to evaluate the resistance to plastic deformation. Due to the lack of crystalline defects in amorphous alloys, their hardness is relatively high compared with the crystalline alloy. From Vickers hardness measurement, it is found that the addition of Ni markedly increases the hardness of the alloy. The cause may be that the free volume in the alloy decreases due to the faster diffusion of Ni than that of Co on cooling. Figure 10 shows the hardness of the alloys annealed under different conditions. From Fig. 10(a), the hardness of these samples abruptly increases by annealing at 823 K for 10 min. The value of hardness was taken from the average of 10 measurements. Because no crystallization is observed from XRD patterns at 823 K for 10 min, this hardening effect should be attributed to the structural relaxation, which leads to the reduction of free volume in the alloy. However, the values of hardness in the alloys with 3% and 5% Ni additions inversely decrease with the increase of annealing time. Obviously, the alloys containing 3% and 5% Ni have lower values of T_g (see Table 1). Thus, the energy for activating atoms in these two alloys (more unstable) is greater than that in others when annealed at the same temperature, and crystallization primarily occurs in these two alloys. At higher annealing temperature of 848 K, the values of hardness in the alloys with 3% and 5% Ni additions decrease at the beginning stage as shown in Fig. 10(b). It is because the amorphous phase in these two alloys directly crystallizes without the process of structural relaxation at such a high temperature. Figure 10(c) presents the temperature-

dependence of the hardness within the whole temperature region. It is obvious that the variation of hardness can be divided into three stages, namely increasing by structural relaxation, decreasing by initial crystallization and increasing by further crystallization. The first two stages have been discussed before. At the third stage, the hardness of these alloys rapidly increases when the annealing temperature is above T_x. According to the XRD patterns, this hardening effect is contributed to the precipitation of carbide and boride such as $(Fe,Ni,Mo)_{23}(B,C)_6$, $(Fe,Cr)_{23}(C,B)_6$ and $(Fe,Cr)_7C_3$, as the annealing temperature increases. The refinement of the grain and the mixture of different compounds make the crystalline state even harder than the amorphous state for these alloys.

3.5 Magnetic properties

The $Fe_{41}Co_7Cr_{15}Mo_{14}C_{15}B_6Y_2$ BMG does not show soft magnetic behavior and exhibits paramagnetic state at room temperature as the former reports [7,13]. The addition of Ni does not change the magnetic properties of these BMGs. However, the experimental results show that the annealing temperature has a remarkable effect on the magnetic properties of these alloys. In the temperature range from 298 K to 893 K, the $Fe_{41}Co_{7-x}Ni_xCr_{15}Mo_{14}C_{15}B_6Y_2$ (x=0, 1, 3, 5) alloys represent the stable paramagnetic state. When the annealing temperature was over 893 K, the alloys gradually shifted from paramagnetic to ferromagnetic state with the increase of temperature. This magnetic transformation, however, could be suppressed by the increasing addition of Ni. The hysteretic loops of the alloys annealed at 1273 K after full crystallization are shown in Fig.11, which indicates that the alloys containing 0−3% Ni exhibit ferromagnetic state, whereas the alloy containing 5% Ni still exhibits paramagnetic state. According to the results of isothermal experiment, the alloys are composed of carbides and borides like $(Fe,Ni,Mo)_{23}(B,C)_6$, $(Fe,Cr)_{23}(C,B)_6$, $(Fe,Cr)_7C_3$, after full crystallization. The solid solubility and grain size of carbides and borides could be remarkably influenced by alloying elements, e.g., Ni and Co, and on the other hand, the magnetic properties of the alloy are closely relative to the composition and grain size of these carbides and borides. The reason of magnetic transformation affected by alloying addition can be summarized as follows. 1) The addition of Ni reduces the solid solubility of Fe in carbide phase such as $M_{23}C_6$ and M_7C_3. The excess Fe, in turn, promotes the precipitation of other nonmagnetic phases like austenite. 2) Ni affects the stabilization of paramagnetic phase by reducing M_s point [26−28]. Based on these two reasons, thus, the alloy can transfer from ferromagnetic to paramagnetic state.

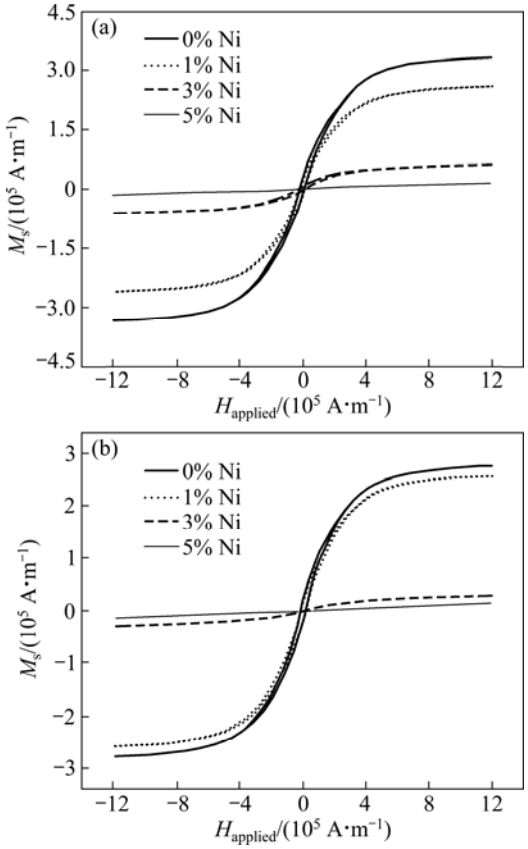

Fig. 11 Hysteresis loops of $Fe_{41}Co_{7-x}Ni_xCr_{15}Mo_{14}C_{15}B_6Y_2$ (x=0, 1, 3, 5) alloys under condition of quenching (a) and annealing (b) at 1273 K

4 Conclusions

1) The value of ΔT_x firstly decreases by adding 1% Ni and then increases to nearly original value by the further addition of Ni. The addition of Ni does not play a positive role for enlarging ΔT_x. However, the alloy with 1% Ni addition, which has the minimum γ and the narrowest ΔT_x, presents the largest value of activation energy at the first step of crystallization.

2) The minor addition of Ni can refine the crystal grain obtained from the full crystallization experiment.

3) The addition of Ni markedly increases the hardness of the alloy. The variation of hardness can be divided into three stages, namely increasing by structural relaxation, decreasing by initial crystallization and increasing by further crystallization.

4) The annealing temperature has a remarkable effect on the magnetic properties of these alloys. The magnetic transformation of alloy could be suppressed by the increasing addition of Ni.

References

[1] LI F S, ZHANG T, GUAN S K, SHEN N F. Crystallization kinetics

and induced magnetic properties of bulk (Fe,Co)−Zr−Nd−B metallic glass [J]. The Chinese Journal of Nonferrous Metals, 2004, 14: 840−845. (in Chinese)
[2] PANG S J, ZHANG T, ASAMI K, INOUE A. New Fe−Cr−Mo−(Nb,Ta)−C−B glassy alloys with high glass-forming ability and good corrosion resistance [J]. Materials Transactions, 2001, 42: 376−379.
[3] LU Z P, LIU C T, CARMICHAEL C A, PORTER W D, DEEVI S C. Bulk glass formation in an Fe-based Fe−Y−Zr−M (M=Cr, Co, Al)−Mo−B system [J]. Journal of Materials Research, 2004, 19: 921−929.
[4] QIU K Q, TA N, SUO Z Y, REN Y L. Glass forming ability and mechanical properties of Fe-based amorphous alloys [J]. The Chinese Journal of Nonferrous Metals, 2008, 18: 614−619. (in Chinese)
[5] STOICA M, ECKERT J, ROTH S, YAVARI A R, SCHULTZ L. FeCrMoGaPCB BMGs: sample preparation, thermal stability and mechanical properties [J]. Journal of Alloys and Compounds, 2007, 434: 171−175.
[6] LU Z P, LIU C T, THOMPSON J R, PORTER W D. Structural amorphous steels [J]. Physical Review Letters, 2004, 92: 245503-1−245503-4.
[7] SHEN J, CHEN Q J, SUN J F, FAN H B, WANG G. Exceptionally high glass-forming ability of an FeCoCrMoCBY alloy [J]. Applied Physics Letters, 2005, 86: 151907-1−151907-3.
[8] BASER T A, BARICCO M. Fe-based bulk metallic glasses with Y addition [J]. Journal of Alloys and Compounds, 2007, 434: 176−179.
[9] HABIB K, ELING V, WU C, MOORE K, MEHALIK R. The effect of C and Co additions on the properties of a Fe−B−Si metallic glass [J]. Scripta Metallurgica, 1990, 24: 1057−1062.
[10] GUO S F, LI N, ZHANG C, LIU L. Enhancement of plasticity of Fe-based bulk metallic glass by Ni substitution for Fe [J]. Journal of Alloys and Compounds, 2010, 504: 78−81.
[11] LESZ S, KWAPULINSKI P, NOWOSIELSKI R. Formation and physical properties of Fe-based bulk metallic glasses with Ni addition [J]. Journal of Achievements in Materials and Manufacturing Engineering, 2008, 31: 35−40.
[12] INOUE A, SHINOHARA Y, GOOK J S. Thermal and magnetic properties of bulk Fe-based glassy alloys prepared by copper mold casting [J]. Materials Transactions, 1995, 36: 1427−1433.
[13] PONNAMBALAM V, POON S J. Fe-based bulk metallic glasses with diameter thickness larger than one centimeter [J]. Journal of Materials Research, 2004, 19: 1320−1326.
[14] TAKEUCHI A, INOUE A. Classification of bulk metallic glasses by atomic size difference, heat of mixing and period of constituent elements and its application to characterization of the main alloying element [J]. Materials Transactions, 2005, 46: 2817−2829.
[15] JOHNSON W L. Bulk glass-forming metallic alloys: Science and technology [J]. MRS Bulletin, 1999, 24: 42−56.
[16] WANIUK T A, SCHROERS J, JOHNSON W L. Critical cooling rate and thermal stability of Zr−Ti−Cu−Ni−Be alloys [J]. Applied Physics Letters, 2001, 78: 1213−1215.
[17] INOUE A, ZHANG W, ZHANG T, KUROSAKA K. High-strength Cu-based bulk glassy alloys in Cu−Zr−Ti and Cu−Hf−Ti ternary systems [J]. Acta Materialia, 2001, 16: 2836−2844.
[18] DU X H, HUANG J C, LIU C T, LU Z P. New criterion of glass forming ability for bulk metallic glasses [J]. Journal of Applied Physics, 2007, 101: 086108-1−086108-3.
[19] YUAN Z Z, BAO S L, LU Y, ZHANG D P, YAO L. A new criterion for evaluating the glass-forming ability of bulk glass forming alloys [J]. Journal of Alloys and Compounds, 2008, 459: 251−260.
[20] INOUE A. High strength bulk amorphous alloys with low critical cooling rates [J]. Materials Transactions, JIM, 1995, 36: 866−875.
[21] INOUE A, ZHANG T, MASUMOTO T. Glass-forming ability of alloys [J]. Journal of Non-Crystalline Solids, 1993, 156: 473−480.
[22] LU Z P, TAN H, LI Y, NG S C. The correlation between reduced glass transition and the glass forming ability of bulk metallic glasses [J]. Scripta Materialia, 2000, 42: 667−673.
[23] LU Z P, LIU C T. A new glass-forming ability criterion for bulk metallic glasses [J]. Acta Materialia, 2002, 50: 3501−3512.
[24] KISSINGER H E. Reaction kinetics in differential thermal analysis [J]. Analytical Chemistry, 1957, 29: 1702−1706.
[25] DANG S E, ZHANG X H, YAN Z J, YONG H U, HAO W X. Correlation between crystallization kinetics of amorphous alloys and primary phases during crystallization [J]. The Chinese Journal of Nonferrous Metals, 2007, 17: 296−302. (in chinese)
[26] BALESTRINO G, CAVALLINI M. Mössbauer spectroscopy study of retained austenite tempering [J]. Scripta Metallurgica, 1983, 17: 1407−1412.
[27] KAPLOW R, RON M, DECRISTOFARO N. Mössbauer effect studies of tempered martensite [J]. Metallurgical Transactions A, 1983, 16: 1135−1145.
[28] MATHALONE Z, RON M, PIPMAN J, NIEDZWIEDZ S. Mössbauer characteristics of ε, χ, and θ iron carbides [J]. Journal of Applied Physics, 1971, 42: 687−695.

Fe−Co−Ni−Cr−Mo−C−B−Y 系大块金属玻璃的热稳定性、晶化行为、维氏硬度和磁性能

韩佳甲[1]，王翠萍[1]，寇生中[2]，刘兴军[1]

1. 厦门大学 材料学院 材料科学与工程系，厦门 361005；
2. 兰州理工大学 有色金属合金及加工教育部重点实验室，兰州 730050

摘 要：研究 $Fe_{41}Co_{7-x}Ni_xCr_{15}Mo_{14}C_{15}B_6Y_2$($x$=0,1,3,5)大块金属玻璃的热稳定性、晶化行为、维氏硬度和磁性能。通过铜模铸造法制备 $Fe_{41}Co_{7-x}Ni_xCr_{15}Mo_{14}C_{15}B_6Y_2$($x$=0,1,3,5)大块金属玻璃。利用差示扫描量热法和等温热处理法研究这些金属玻璃的热稳定性和晶化行为。在室温下利用维氏硬度计测量试样经过不同温度和时间退火后的硬度，并对它们的磁学性质进行表征。实验结果表明，少量 Ni 元素的加入没有增大过冷液相区间和玻璃形成能力，但是改变合金的初始晶化行为，增大晶化激活能。少量 Ni 元素的加入能够细化最终晶化组织中的晶粒大小。初晶相使合金的硬度降低，但随着热处理温度的升高，所有合金的硬度都明显提高，原因是析出了大量的碳化物和硼化物。退火温度对合金的磁性能有很大影响，少量 Ni 元素的加入阻止了合金在高温退火后从顺磁态向铁磁态的转变。

关键词：Fe−Co−Ni−Cr−Mo−C−B−Y；金属玻璃；热稳定性；退火；磁性能

(Edited by Sai-qian YUAN)